

# Comparison of the fit and geometry of reconstruction of femoral components of four cemented canine total hip replacement implants

Kurt S. Schulz, DVM, MS; Cheri Nielsen, BS; Susan M. Stover, DVM, PhD; Philip H. Kass, DVM, PhD

**Objective**—To compare fit and geometry of reconstruction of femoral components of 4 canine cemented total hip replacement implants and determine which implants are most compatible with current principles of cemented arthroplasty.

**Sample Population**—Paired femurs from 16 adult mixed-breed dogs.

**Procedure**—Femurs were prepared for femoral stem implantation of either the Bardet, BioMedtrix, Mathys, or Richards II implant. Mediolateral and cranio-caudal radiographs were obtained with femoral components in situ. Cross-sectional analysis of implant fit was performed on transected cemented specimens. Computer-aided analyses of digitized images were performed.

**Results**—The Bardet and Richards II implants reconstructed the original femoral head position significantly better than the other 2 implants. None of the implants allowed neutralization of the implant axis in the sagittal plane or were routinely centralized in the femoral canal. The Bardet implant had the smallest minimum distal tip offset in the sagittal plane. Greatest tip to cortex distance was provided by the Richards II implant in the transverse plane and the Mathys implant in the sagittal plane. The thinnest cement mantle regions for all implants were in the central longitudinal third of the femoral stem.

**Conclusions and Clinical Relevance**—The Bardet and BioMedtrix implants had stem design characteristics that were most compatible with principles of cemented stem fixation. None of the implants completely satisfied the theoretically optimal conditions of centralization and neutralization of the femoral stem. Innovative design modifications, therefore, may be needed if these conditions are important to the long-term success of canine total hip replacement. (*Am J Vet Res* 2000;61:1113–1121)

Aseptic loosening is one of the leading causes of failure of cemented total hip replacements in dogs.<sup>1</sup> In humans and dogs, this mechanism of failure appears to be more commonly associated with the femoral component than the acetabular component and likely involves mechanical failure of the

cement-implant interface.<sup>2,3</sup> The durability of the femoral cement-implant interface depends on the surgical implantation technique and implant design. Both of these factors affect the fit of the implant within the femoral canal and the geometry and kinematics of the reconstructed femur.<sup>4</sup> Implant fit and geometry of reconstruction subsequently affect the longevity of the replacement and, therefore, the long-term success of the procedure.<sup>2,3,5</sup> In addition, implant design also affects the ease of surgical implantation. Ultimately, all of these factors appear to have effects on the long-term success of total hip arthroplasty.

There are currently few commercially available canine total hip replacement systems. Unlike human medicine, veterinary surgeons usually have only one implant system for all of their canine patients. It is important, therefore, that the implant system has design characteristics that, for a spectrum of patients, will minimize stress riser effects and wear products, maximize cement-implant interface strength, reconstruct normal geometric features of the proximal portion of the femur, prevent cement failure, and facilitate surgical implantation. Four designs of commercially available canine total hip replacement implants include the Richards II,<sup>a</sup> BioMedtrix,<sup>b</sup> Mathys,<sup>c</sup> and Bardet.<sup>d</sup> The Richards II is a cobalt-chrome nonmodular collared prosthesis. The Bardet implant is a machined titanium modular collared stem with a smooth nonpolished surface, antirotational grooves, and cobalt-chrome head. The BioMedtrix is a cast cobalt-chrome modular collared prosthesis with a grit-blasted proximal third and antirotational grooves. The Mathys is a forged 316L stainless steel nonmodular prosthesis with a bead-blasted rectangular stem.

The purpose of the study reported here was to compare fit and geometry of reconstruction of femoral components of 4 canine cemented total hip replacement implants and determine which implants are most compatible with current principles of cemented arthroplasty.

## Materials and Methods

**Study design**—Paired femora selected to accept a uniform femoral implant size were obtained from cadavers of 16 adult mixed-breed dogs and systematically prepared for implantation of canine cemented femoral stem prostheses of 4 designs. Geometry of reconstruction and implant fit were evaluated in the transverse and sagittal planes by computerized geometric analysis of radiographs of implanted specimens. Implant fit and cement mantle thick-

Received Apr 26, 1999.

Accepted Aug 31, 1999.

From the JD Wheat Veterinary Orthopedic Research Laboratory, School of Veterinary Medicine, University of California, Davis, CA 95616.

Supported by the Center for Companion Animal Health, University of California, Davis, CA 95616.

ness were determined in the horizontal plane using specimen cross-sectional analysis after optimum implant centralization.

**Specimen preparation**—Femurs were collected from 16 mixed-breed dogs (body weight > 22 kg) euthanatized for reasons unrelated to this study. Because the dogs were obtained from a humane society, signalment and history were not available. All dogs were judged to be skeletally mature on the basis of radiographic evidence of complete femoral growth plate closure. Soft tissues were removed from the bones by manual dissection, and specimens were stored at -20 C in sealed waterproof bags. Specimens were returned to 21 C prior to further manipulation. Each femur was mounted in a clear plastic orthogonal frame with transverse plane leveling on the basis of a modification of the technique described by Ruff et al.<sup>6</sup> Briefly, positioning was standardized by placing the distal aspects of both femoral condyles in contact with the X-Y plane of the orthogonal frame (Fig 1). Transverse leveling was achieved by elevating the medial aspect of the lesser trochanter and the medial aspect of the lateral supracondylar tubercle equidistant above the X-Z plane.

Lateromedial and craniocaudal radiographs (54 kV; 1.7 mA) of each femur in the orthogonal frame were obtained with a magnification indicator at the level of the longitudinal axis of the diaphysis. The X-Z or Y-Z plane of the frame was elevated 10 cm above the table to achieve 115% magnification. Radiographic image magnification of 115% was confirmed by measurement of the magnification indicator, permitting comparison of the femoral radiographs with a femoral stem radiograph template<sup>8</sup> for prosthesis size selection. Femoral stem size was selected to yield an estimated cement mantle of 2 mm around the distal third of the implant by use of the BioMedtrix template system. Radiographs and gross specimens were examined, and specimens were discarded if found to have evidence of previous trauma or disease. Sixteen pairs of femurs identified as accepting a size-8 BioMedtrix stem were used in the study. Pairs of femora were randomly separated into 2 groups. Each of the 4 stem designs was then designated for implantation in the left or right femurs of 1 of the 2 groups.

Steel balls (1 mm diameter), serving as radiographic markers, were cemented with cyanoacrylate into superficial drill holes (1.5 mm diameter) at the most prominent point of the lesser trochanter and the most prominent point of the lateral supracondylar tubercle of each specimen. Radiographs were repeated as described.

Four implant designs were tested (Fig 2). Implant size was selected on the basis of the manufacturers' recommendations and the ability to achieve a 2-mm-thick cement

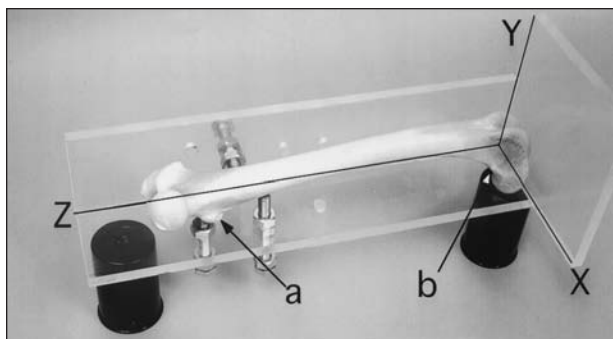


Figure 1—Oblique view of an intact femur from a canine cadaver, positioned in an orthogonal frame with identification of the various planes (X, Y, and Z). a = Lesser trochanter. b = Lateral supracondylar tubercle.

mantle around the distal third of the implant, with the exception of the Mathys implant. Implant size for the Mathys implant was selected on the basis of maximizing direct medial and lateral endosteal-implant contact while maintaining a 2-mm minimum cement mantle on the cranial and caudal surfaces of the implant. Femoral specimens were prepared for femoral stem implantation as described by the manufacturers of the 4 femoral implants. The **sagittal diaphyseal axis (SDA)** was permanently etched on the cranial surface of each specimen.<sup>3</sup> The SDA was determined on each specimen by identifying the external diaphyseal mediolateral isthmus and connecting the midpoints of transverse lines 20 mm proximal and distal to the isthmus to generate a line the entire length of the femur. Femoral head and neck osteotomies were performed at the level of the lesser trochanter by placing a steel osteotomy template on the SDA and aligning the cut level such that the osteotomy line would intersect the lesser trochanter (Fig 3). Steel osteotomy templates used were specific to each of the femoral stems to be implanted.

After osteotomy, all femora were routinely prepared by one investigator (CN), using instrumentation of the appropriate size and type, as described by the manufacturer of each implant. Preparation of the femoral bone canal included low-speed (150-rpm) drilling with a No. 8 drill bit for all groups, low-speed reaming, seating the reamer to the level of cut, and manual broaching. Initially, each specimen was broached to the point that the broach was seated level with the osteotomy site; however, if the implant did not seat completely, further broaching was performed just until the collar of the implant would rest on the osteotomy site.



Figure 2—Media (upper row) and cranial (lower row) views of 4 canine cemented femoral implant stems evaluated for fit and geometry of reconstruction. A = BioMedtrix.<sup>b</sup> B = Bardet.<sup>d</sup> C = Richards II.<sup>a</sup> D = Mathys.<sup>c</sup>

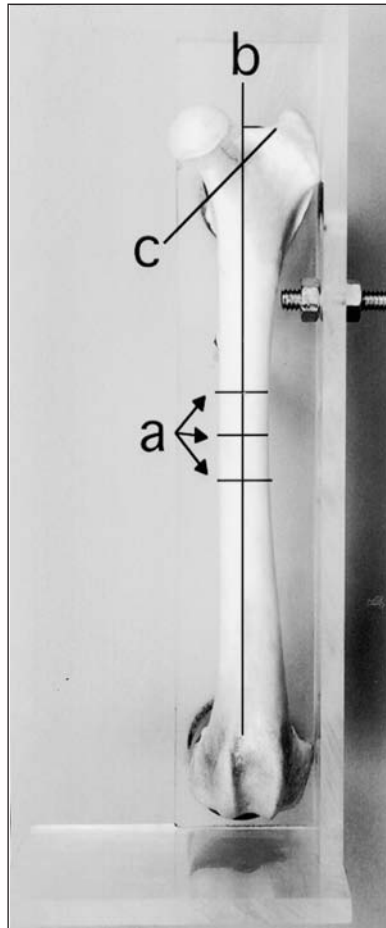


Figure 3—Cranial view of an intact femur from a canine cadaver, in an orthogonal frame. a = Location of isthmus and parallel lines located 20 mm proximal and distal to the isthmus. b = Sagittal diaphyseal axis. c = Site of lesser trochanteric osteotomy.

Each femoral prosthesis was implanted in normoverision in the assigned specimen in the orthogonal frame. The BioMedtrix rigid centralizing device was used with the BioMedtrix implant. Modular components were radiographed with the shortest femoral heads in place. For each specimen, the femoral implant was put in 4 positions maintained by use of modeling clay. All implant positioning was performed by one person (CN). Initially, the implant was placed with maximal cranial tipping of the distal aspect of the implant, and a mediolateral radiograph was obtained. Radiographs of each specimen were repeated after maximal caudal tipping of the distal aspect of the implant. The orthogonal frame and femur were then rotated 90° for subsequent craniocaudal radiographs. Each specimen was subsequently radiographed in a craniocaudal view with the implant tip in maximum valgus and maximum varus positioning.

Each femur was then transected at a level approximately 1 cm distal to the distal-most aspect of the femoral component of the implant. The vertical position of the distal tip of the implant was determined with a depth gauge and etched on the external cortex. Using a standard technique, 2.7-mm bone screws were inserted at the level of the distal aspect of the femoral component of the implant on the cranial, caudal, medial, and lateral surfaces of each bone. Screw depth was adjusted with the femoral component in place, to achieve tip centralization by establishing equal distances, at the distal level of the implant, between the implant and the endosteum on the medial and lateral sides and on the cranial and caudal sides (Fig 4). For this portion of the study, the BioMedtrix implant was used

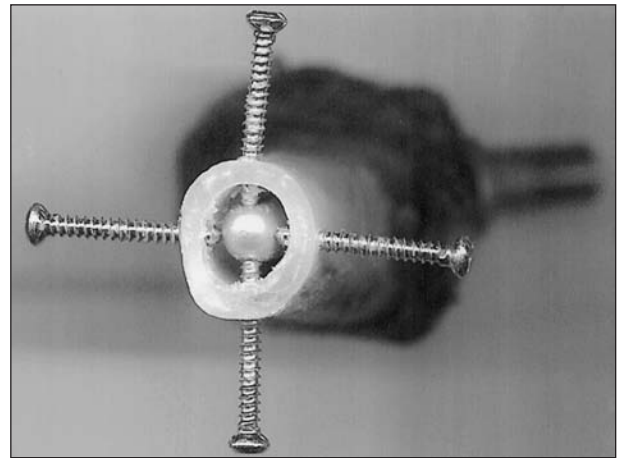


Figure 4—View of distal aspect of a canine femur after transection at the level of the distal tip of the femoral stem implant and centralization of the distal tip with bone screws.

without the rigid centralizing device. The femoral stems were removed, and the screws were left in place to centralize the stem during cementing. The femora were subsequently filled with colored bone cement by use of a standard clinical technique and the corresponding femoral stem component was coated with lubricant and reimplanted into the cement-filled specimen. After the cement hardened, the femoral components and screws were removed and the resulting void was filled with contrasting uncolored bone cement. Each specimen was cut into 5-mm-thick slices on a plane perpendicular to the SDA by use of a sectioning system for undecalcified tissues and metallic implants.<sup>6</sup> Sectioning was performed from distal to proximal, beginning at the position of the distal tip of the implant.

**Radiographic analysis**—Radiographs were processed automatically, digitized,<sup>6</sup> cropped,<sup>8</sup> and imported to drafting software<sup>h</sup> for axis application and measurement.

**Sagittal plane imaging**—The transverse diaphyseal axis (TDA) was generated on each lateral image. A line was drawn at the outer cortical surface, connecting the radiographic markers positioned at the lesser trochanter and supracondylar tubercle. A proximal diaphyseal circle was generated by use of a modified symmetrical axis technique, at the level of the lesser trochanter.<sup>7</sup> A distal diaphyseal circle was generated on a line perpendicular to the marker line and 8 cm distal to the proximal circle. The centers of the 2 circles were connected to generate the TDA. The TDA used in the study reported here was not intended to be a biomechanical or volumetric axis but to represent the recommended axis for implant positioning. The center of the femoral head was identified by use of a best fit circle method. Femoral head offset was determined on images of intact specimens by measuring the distance from the center of the femoral head to the TDA on a line perpendicular to the TDA. Femoral head position was determined by measuring the distance from the center of the femoral head to the level of the lesser trochanter on a line parallel to the TDA.<sup>8,9</sup>

On images of implanted specimens, the axis of the femoral implant was generated by applying a symmetrical axis technique to the implant stem. Measurements made on images of implanted specimens included minimum stem angulation and variability of stem angulation, minimum distal tip offset and variability of distal tip offset, minimum and maximum tip to caudal cortex distance (TCD), femoral

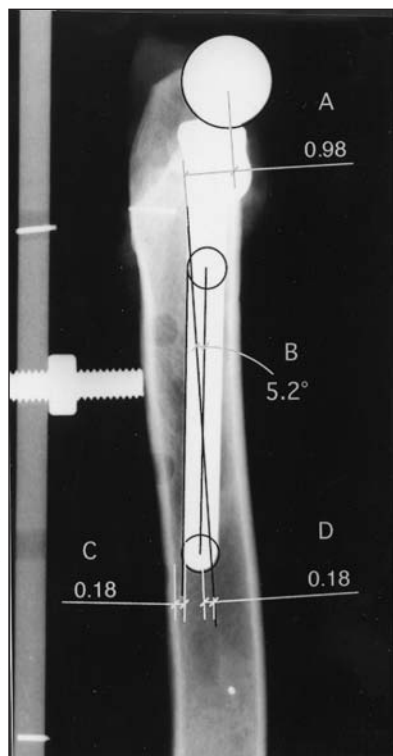


Figure 5—Mediolateral radiographic view of a canine femur after implantation of a femoral component. Measurements depicted include femoral head offset (A; cm), stem angulation (B), tip-to-caudal cortex distance (C; cm), and offset of the distal aspect of the stem (D; cm).

head offset, and femoral head position (Fig 5). Stem angulation was defined as the degree and direction (cranial or caudal) from the implant axis to the TDA. Distal stem offset was defined as the distance and direction (cranial or caudal) from the implant axis to the TDA on a line perpendicular to the implant axis at the distal most aspect of the implant. Tip to caudal cortex distance was determined by measuring the distance from the caudal margin of the distal most aspect of the implant to the endosteal surface of the caudal cortex on a line perpendicular to the implant axis.

**Transverse plane imaging**—The SDA was generated on each craniocaudal image in a method similar to that of the TDA. On images of intact specimens only, the femoral head offset was calculated. On images of implanted specimens, the axis of the femoral implant was similarly generated by applying a modified symmetrical axis technique to the implant stem. Measurements made on images of implanted specimens included minimum and variability of stem angulation, minimum and variability of distal tip offset, minimum and maximum TCD, and femoral head offset.

**Cross-section analysis**—The proximal surface of the cross-sectional specimen slices were photographed with an in-frame scale, and the photographic slides were digitized.<sup>1</sup> A radial grid was applied to the image of each slice, centering the grid on the center of the cement representing the implant (Fig 6). The cement mantle thickness was measured on each of 8 equidistant radial axes, and locations of cement mantle thickness < 2 mm were recorded.

**Data reduction**—An implant was considered centralizable in the sagittal plane if the distal stem offset range delineated by the maximum cranial and maximum caudal limits included zero. An implant was considered centralizable in the transverse plane if the distal stem offset range delineated by the maximum valgus and maximum varus limits included zero. Stem angle was considered neutralizable in the sagittal or transverse plane if the stem angle ranges delineated by the

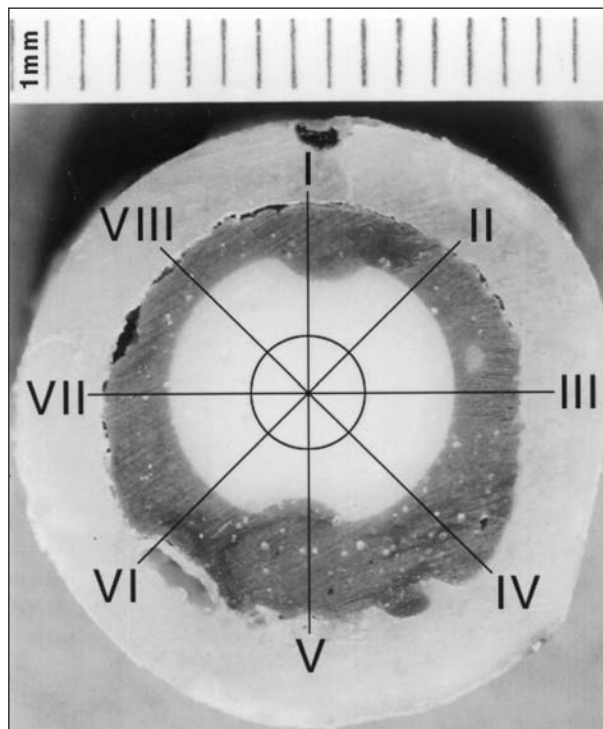


Figure 6—Computer image of cross-sectional slice of a canine femur after cemented implantation of a femoral stem and subsequent replacement of the stem with contrasting bone cement. A computerized axial grid (Roman numerals) is applied for measurement of cement thickness.

maximum cranial and caudal or valgus and varus limits, respectively, included zero. An implant was considered to have forced tip contact in a plane if the distance between the implant tip and adjacent cortex was zero, regardless of implant position.

The femoral head offsets for all available femoral head lengths of modular implants were compared for each position of each specimen. Femoral head offsets for head lengths not radiographed were determined by computer simulation of those head lengths on the scanned radiographs. The femoral head length providing the closest head offset and position to that of the intact specimen was recorded as the optimal head length. The femoral head offset and position for each specimen fitted with its optimal length head was then compared with the femoral head offset and position of the intact specimen to determine the mean difference for each implant design.

**Statistical evaluation**—Effects of implant design on ability to reconstruct original femoral head offset and position and centralization of the distal implant tip were evaluated by use of exact logistic regression. Effect of implant design on ability to achieve a neutral implant angle, forced tip contact, and ability to achieve a 2-mm tip-to-cortex distance were also evaluated by use of exact logistic regression. Results are presented as odds ratios, associated 95% confidence intervals, and exact mid-values for *P*. Analysis of variance was used to compare minimum distal stem offset and variability, minimum stem angulation and variability, and minimum and maximum tip with caudal cortex distance. Significance was set at *P* < 0.05.

## Results

**Effect of implant design on femoral head offset and position**—Original femoral head offset in the transverse plane was reconstructed most closely by the

Table 1—Difference of femoral head position and offset (cm) between intact canine femurs and femurs that received implantation of a cemented femoral stem implant

Implant	Position	Transverse offset	Sagittal offset
Bardet			
Mean (SD)	0.31 <sup>a</sup> (0.27)	0.81 <sup>c</sup> (0.13)	0.23 <sup>a</sup> (0.21)
Median	0.20	0.80	0.20
BioMedtrix			
Mean (SD)	0.81 <sup>b</sup> (0.14)	1.20 <sup>d</sup> (0.10)	0.28 <sup>a</sup> (0.20)
Median	0.80	1.20	0.28
Mathys			
Mean (SD)	0.90 <sup>b</sup> (0.23)	0.94 <sup>c,d</sup> (0.17)	0.3 <sup>a</sup> (0.19)
Median	0.80	1.00	0.25
Richards II			
Mean (SD)	0.31 <sup>a</sup> (0.20)	0.88 <sup>c,d</sup> (0.14)	0.26 <sup>a</sup> (0.25)
Median	0.25	0.93	0.20

<sup>a-e</sup>Mean values with different superscripts within a column are significantly ( $P < 0.05$ ) different.

Bardet implant (mean difference of reconstruction, 0.81 cm), although difference from other implants was only significant for the BioMedtrix implant (mean difference of reconstruction, 1.2 cm; Table 1). Original femoral head offset in the sagittal plane was also reconstructed most closely by the Bardet implant (mean difference of reconstruction, 0.23 cm); however, this was not significantly different from the offset reconstruction of any of the other implants. The Bardet and Richards II implants provided the best reconstruction of femoral head position (mean difference of reconstruction, 0.31 cm) and were significantly closer in reconstruction than the Mathys and BioMedtrix implants.

**Effect of implant design on stem angulation—**Significant differences were not detected among femoral stem designs in minimum possible angle between the implant and the femoral diaphysis in the transverse or sagittal planes (Tables 2 and 3). None of the implants allowed complete neutralization of the implant axis in the sagittal plane. The Bardet implant provided the greatest available variability in implant angulation in the transverse plane but not significantly greater than any of the other specimens tested. The Mathys implant provided the greatest available variability in implant angulation in the sagittal plane but was not statistically greater than those of the other implants.

**Effect of implant design on distal tip offset—**Significant differences were not detected among implants in minimum distal tip offset in the transverse plane; however, in the sagittal plane, the Bardet implant provided the smallest minimum distal tip offset (mean, 0.1 cm), which was significantly better than that of the Richards II implant (mean, 0.24 cm; Tables 2 and 3). The Bardet implant provided the greatest available variability of distal tip offset in the transverse plane (mean, 0.3 cm), which was significantly greater than that of the Richards II implant. Significant differences among implants for odds of achieving centralization in either plane were not detected (Tables 4 and 5).

**Effect of implant design on TCD—**The Richards

Table 2—Measurements of fit in the transverse plane for 4 canine cemented femoral stem implants

Implant	Minimum angle (degrees)	Angle variability (degrees)	Minimum distal tip offset (cm)	Distal tip offset variability (cm)	Minimum tip to cortex distance (cm)
Bardet					
Mean (SD)	3.51 <sup>a</sup> (1.33)	1.87 <sup>b</sup> (0.98)	0.06 <sup>d</sup> (0.05)	0.30 <sup>e</sup> (0.26)	0.09 <sup>g</sup> (0.03)
Median	3.30	1.80	0.10	0.20	0.10
BioMedtrix					
Mean (SD)	3.20 <sup>a</sup> (0.98)	0.66 <sup>b</sup> (0.65)	0.02 <sup>d</sup> (0.05)	0.09 <sup>e,f</sup> (0.10)	0.104 <sup>g</sup> (0.05)
Median	3.20	0.55	0.00	0.10	0.10
Mathys					
Mean (SD)	4.59 <sup>a</sup> (1.47)	1.37 <sup>b</sup> (0.92)	0.06 <sup>d</sup> (0.07)	0.16 <sup>e,f</sup> (0.13)	0.10 <sup>g</sup> (0.07)
Median	4.45	1.64	0.05	0.15	0.10
Richards II					
Mean	2.77 <sup>a</sup> (1.29)	0.70 <sup>b</sup> (0.60)	0.06 <sup>d</sup> (0.07)	0.06 <sup>f</sup> (0.07)	0.26 <sup>h</sup> (0.05)
Median	2.80	0.60	0.05	0.05	0.30

<sup>a-h</sup>Mean values with different superscripts within a column are significantly ( $P < 0.05$ ) different.

Table 3—Measurements of fit in the sagittal plane for 4 canine cemented femoral stem implants

Implant	Minimum angle (degrees)	Angle variability (degrees)	Minimum distal tip offset (cm)	Distal tip offset variability (cm)	Minimum tip to cortex distance (cm)
Bardet					
Mean (SD)	4.07 <sup>a</sup> (0.86)	0.86 <sup>b</sup> (0.80)	0.10 <sup>c</sup> (0.05)	0.11 <sup>e</sup> (0.08)	0.20 <sup>f,g</sup> (0.18)
Median	4.05	0.75	0.10	0.10	0.20
BioMedtrix					
Mean	4.10 <sup>a</sup> (1.36)	0.59 <sup>b</sup> (0.60)	0.11 <sup>c,d</sup> (0.08)	0.07 <sup>e</sup> (0.09)	0.12 <sup>f,g</sup> (0.05)
Median	4.00	0.40	0.10	0.05	0.10
Mathys					
Mean	4.93 <sup>a</sup> (1.35)	1.25 <sup>b</sup> (1.16)	0.12 <sup>c,d</sup> (0.07)	0.16 <sup>e</sup> (0.14)	0.26 <sup>f</sup> (0.07)
Median	5.30	0.95	0.10	0.15	0.25
Richards II					
Mean	4.77 <sup>a</sup> (1.25)	0.52 <sup>b</sup> (0.64)	0.24 <sup>d</sup> (0.11)	0.50 <sup>e</sup> (0.11)	0.12 <sup>g</sup> (0.17)
Median	5.05	0.35	0.25	0.00	0.10

<sup>a-g</sup>Mean values with different superscripts within a column are significantly ( $P < 0.05$ ) different.

Table 4—Odds ratios (OR), 95% confidence intervals (95% CI), and *P* values for effects of 4 canine cemented total hip replacement femoral implant stems on forced contact between the distal implant tip and the endosteal surface (FC), ability to centralize the distal implant tip (C), and ability to achieve a distal cement mantle of 2 mm (2-mm CM) in the transverse plane

Variable	Implant	OR	95% CI	<i>P</i> value
FC	BioMedtrix	1.00	NA	NA
	Richards II	Not estimable	Not estimable	Not estimable
	Mathys	2.66	0.19–∞	0.47
	Bardet	1.00	0.026–∞	1.00
C	BioMedtrix	1.00	NA	NA
	Richards II	0.26	0.004–4.40	0.57
	Mathys	0.16	0.0025–2.41	0.28
	Bardet	1.00	0.011–89.65	1.00
2-mm CM	BioMedtrix	1.00	NA	NA
	Richards II	12.44	1.33–∞	0.026
	Mathys	0.58	0.035–7.36	1.00
	Bardet	0.21	0.00–2.21	0.20

NA = Not applicable.

Table 5—Odds ratios, 95% CI, and *P* values for effects of 4 canine cemented total hip replacement femoral implant stems on FC, C, and ability to achieve a distal 2-mm CM in the sagittal plane

Variable	Implant	OR	95% CI	<i>P</i> value
FC	BioMedtrix	1.00	NA	NA
	Richards II	4.87	0.45–∞	0.20
	Mathys	Not estimable	Not estimable	Not estimable
	Bardet	2.66	0.19–∞	0.47
C	BioMedtrix	1.00	NA	NA
	Richards II	0.38	0.00–5.22	0.47
	Mathys	1.00	0.055–18.24	1.00
	Bardet	1.00	0.055–18.24	1.00
2-mm CM	BioMedtrix	1.00	NA	NA
	Richards II	1.00	0.055–18.24	1.00
	Mathys	19.82	2.12–∞	0.01
	Bardet	4.47	0.41–75.82	0.31

NA = Not applicable.

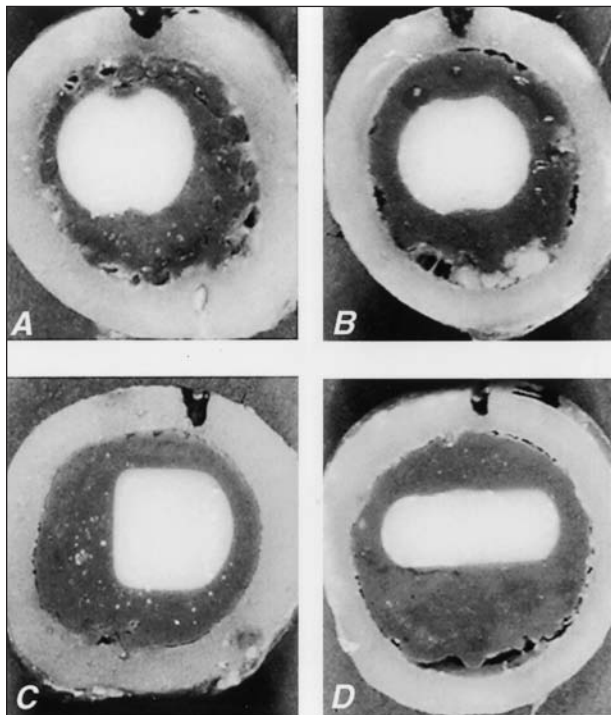


Figure 7—Mid-implant cross-sectional slices of 4 canine cemented femoral implant stems evaluated for fit and geometry of reconstruction. A = BioMedtrix. B = Bardet. C = Richards II. D = Mathys.

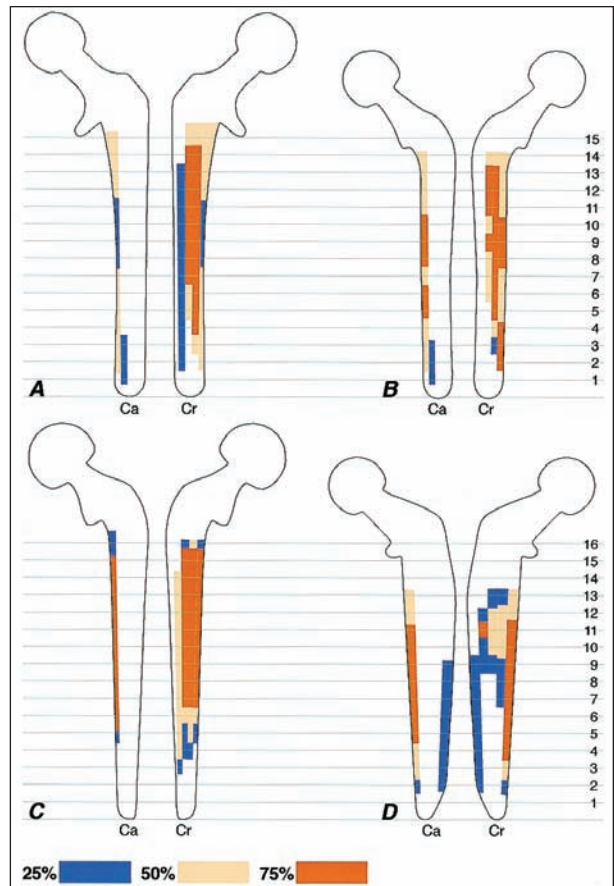


Figure 8—Schematic representations of caudal (Ca) and cranial (Cr) views of 4 canine cemented femoral implant stems, indicating regions of cement mantle where > 25%, 50%, or 75% of the mantle was < 2 mm thick. A = BioMedtrix. B = Bardet. C = Richards II. D = Mathys. Numbers along the right side of the representation indicate levels of sectioning for analysis.

II femoral stem allowed for the greatest minimum TCD in the transverse plane (0.26 mm), which was significantly larger than that of any other implant (Table 2). In the sagittal plane, the Mathys implant provided the greatest minimum TCD (mean, 0.26 mm), which was significantly different only from that of the Richards II implant (Table 3). Significant differences between implants were not detected for odds of forced contact between the distal implant and the cortex in either plane (Tables 4 and 5). Odds of achieving a 2-mm cement mantle in the transverse plane were significantly greater with the Richards II implant than with any other implant. Odds of achieving a 2-mm cement mantle in the sagittal plane were significantly greater with the Mathys implant than with any other implant. Significant differences between odds ratios of the remaining implants were not detected.

**Cross-sectional analysis**—The set screw technique effectively centralized the distal tip of all implants, as indicated by the adequacy of cement thickness (> 2 mm) in the distal sections of all specimens (Fig 7). Thinning of the cement mantle (< 2 mm) occurred most extensively on the craniomedial aspect of the femoral canal for the Richards II, BioMedtrix, and Bardet implants (Fig 8).

Thinning of the cement mantle occurred primarily on the medial aspect of the femoral canal with the Mathys implant. The most consistent levels of cement mantle thinning were sections 7 through 14 for all of the implants. The Richards II implant had the greatest number of cement measurements under 2-mm thickness, whereas the Mathys implant had the fewest.

## Discussion

Substantial design differences are evident among the 4 canine cemented total hip replacement systems tested in the study reported here, including materials, manufacturing, finishing, modularity, shape, and anchoring mechanism. In a comparison of the ability of the 4 implants to reconstruct original geometric features of the proximal portion of the femur, few significant differences were identified; the Bardet implant provided the most anatomically correct reconstruction. In comparison of measurements of implant fit, the Bardet implant provided the smallest distal stem offset in the sagittal plane. None of the implants allowed for complete neutralization of the implant axis in the sagittal plane, and only marginal differences in stem neutralization in the transverse plane were detected. Tip to cortex distance was maximized by the Richards II implant in the transverse plane and by the Mathys implant in the sagittal plane.

Differences identified in the study reported here are a function of the variations in femoral stem shape. Total hip replacement stems should adequately reconstruct geometry of the proximal portion of the femur to restore normal joint kinematics.<sup>5</sup> Stem shape must also minimize risk of implant failure attributable to fatigue, cement failure associated with stress risers, and bone loss attributable to stress shielding.<sup>10-12</sup> The specific factors of implant positioning that are thought to affect implant fixation include neutralization of the angle between the axis of the implant and the axis of the femoral diaphysis, centralization of the distal tip of the implant, and maintenance of a 2-mm-thick cement mantle surrounding the distal third of the stem.<sup>2</sup> The stem should be shaped to allow ease of surgical implantation to permit ideal implant positioning.<sup>4</sup>

The Richards II implant was the first commercially available canine total hip replacement implant to have widespread clinical application. Although the implant is no longer readily available, it was evaluated in our study as a means of comparison because of its presumed ease of insertion and centralization and excellent reconstruction of normal geometric features of the proximal portion of the femur. The excellent ability of the Richards II to reconstruct the geometric features of the proximal portion of the femur was confirmed in our study and indicates that femoral head modularity is not uniformly necessary for accurate geometric reconstruction. The Richards II implant required the least preparation of the femoral canal and was the easiest of the implants to insert. This is likely attributable to the compact nature of the stem. The Richards II stem is sharply tapered and has a flat lateral surface and rounded medial surface. This shape resulted in generally poor tip positioning and cement

mantle thickness in the sagittal plane and excellent tip positioning and cement mantle thickness in the transverse plane. Results of cross-sectional analysis indicated that this implant also had the greatest overall number of cement mantle measurements < 2 mm of thickness. This is likely attributable to the rectangular cross-sectional shape of the stem that results in thinning of the cement between the longitudinal implant edges and the femoral cortex. In addition, the acute distal tip and relatively sharp lateral edges are probable stress risers that are more likely to initiate cement cracking than more rounded designs. On basis of these findings, the cross-sectional design of the Richards II is not highly compatible with contemporary cementing principles and may not be ideal for routine use in canine total hip replacement.

The nonmodular design of the Mathys implant provided femoral head offset similar to other implants but with significantly worse femoral head positioning, suggesting the necessity for either modification in the angle or length of the neck of the implant or modification in the location of femoral head osteotomy when using this implant. The narrowness of the stem in the sagittal plane resulted in increased available angulation and provided the greatest TCD of any of the implants tested. This is likely of clinical importance, because contact of the implant tip with the caudal cortex and thinning of the cement mantle in this region have been reported as common implant malpositions in clinical canine total hip replacement.<sup>13</sup> In the transverse plane, the blade-like design of the Mathys implant is designed to have implant-bone contact on the medial and lateral aspects. Load transfer from this implant to the femur is intended to occur through a cement mantle on the cranial and caudal surfaces and directly from the implant to the bone on the medial and lateral surfaces. The biomechanical efficacy of this unusual design has not been reported in the literature. In the study reported here, both the radiographic and cross-sectional analyses failed to reveal consistent contact between the medial and lateral surfaces of the stem of the Mathys implant and the cortex. This may be attributable to our inexperience in implant design and specimen preparation for this implant but is more likely a reflection of the limited size variation available with this stem. Inability to achieve contact between the medial and lateral edges and the cortex resulted in regions of extremely thin cement. The decision to use this implant in canine total hip replacement should be made with caution because of the difficulty in achieving contact between the medial and lateral edges and the cortex and the subsequent likelihood of cement failure in these regions.

In the United States, the BioMedtrix total hip replacement system is likely the most widely used system in dogs. We found the BioMedtrix instrumentation system to be, subjectively, the most complete and effective in femoral canal preparation. In addition, this system provides the greatest number of head and stem sizes, enabling the system to be used on a wide variety of patients. The BioMedtrix system was also the only system tested with a centralizing device. Stem design of

the BioMedtrix system resulted in femoral head positioning and offset that was less accurate than was typical for the other implants. The design factors that contribute to accurate geometric reconstruction include femoral neck length and angle. Although the clinical importance of accurate reconstruction of femoral geometric features has not been investigated in dogs, in humans it has been determined to have an effect on kinetic and kinematic function of the coxofemoral joint and may affect the long-term stability of the implant.<sup>5,14</sup> The BioMedtrix implant had measurements of fit that were nearly as good as those of the Bardet implant. The BioMedtrix stem shape minimizes stress risers and has proximal surface roughening to increase bonding between the cement and the stem. These qualities, in combination with the implant fit characteristics identified in the study reported here, suggest that the BioMedtrix implant has stem design characteristics highly compatible with contemporary theories of cemented total hip replacement fixation. An exception to this is the tendency of the implant to caudal tipping, a malposition common to all of the implants evaluated in the study reported here.

The Bardet implant combines a machined titanium modular collared stem with a cobalt-chrome head. Although different metals are rarely combined in orthopedic implants because of concerns for galvanic corrosion, the combination of cobalt-chrome and titanium actually increases resistance to galvanic corrosion because of self-passivation of the titanium alloy.<sup>15</sup> Of all implants tested, the design of the Bardet femoral head and stem resulted in the best overall reconstruction of the geometric features of the proximal portion of the femur. The Bardet implant also provided the best tip centralization in the sagittal plane and the greatest variability in implant angulation and tip location in the transverse plane. Variability in implant positioning is desirable in canine total hip replacement, because stem design alone does not reliably result in ideal implant positioning. The surgeon must be able to manipulate the implant within the femoral canal to optimize implant fit. Results of the study reported here suggest that the Bardet and BioMedtrix implants have stem design characteristics most compatible with contemporary theories of cemented total hip replacement fixation; however, subjectively, the design of instrumentation for the Bardet system made implantation of the stem substantially more difficult than implantation with the BioMedtrix system.

Results of cross-sectional analysis of these implants indicated that the greatest region of cement mantle thinning was in the central vertical third of the stem for all 4 femoral stems. The clinical importance of cement thinning in this region may be minimal, because this region has much lower levels of load transfer and cement stress, compared with the proximal and distal thirds of the implant.<sup>16</sup> The proximal third of the stems had the second greatest extent of cement mantle thinning, primarily in the cranio-medial aspect, for all 4 implants. As indicated by results of previous studies, this is because none of the implants completely reconstruct the femoral neck.<sup>4</sup> Implantation of a prosthesis within the residual

femoral neck forces the proximal aspect of the implant cranially and medially, leading to cement mantle thinning in this region and causing the caudal implant tipping that was apparent with all 4 implants. In collared implants, load transfer between the implant, cement, and bone in the proximal region may be bypassed through load transferred directly from the implant collar to the bone; therefore, thinning of the cement mantle in this region may be tolerated in the presence of a well-seated collar.<sup>16</sup> An adequate cement mantle was maintained surrounding the distal third of the stems for most of the specimens when using the set screw technique. This suggests that adequate cement mantle thickness can be achieved in most instances with the implants tested in our study. Adequacy of cement mantle thickness surrounding the distal third of the femoral stem is vital to the long-term survival of the femur-cement-implant composite because of the high load transfer in this region and the propensity for cement cracking associated with the stress riser of the tip.<sup>2,16</sup>

The Bardet and BioMedtrix implants had stem design characteristics that were most compatible with contemporary principles of cemented stem fixation. None of the implants completely satisfied the theoretically optimal conditions of centralization and neutralization of the femoral stem. Caudal implant tipping was an important malposition associated with all 4 stems. Innovative design modifications, therefore, may be indicated if precise femoral stem positioning is important to the long-term success of total hip replacement in dogs.

<sup>a</sup>Richards II, Richards Mfg, Memphis, Tenn.

<sup>b</sup>Modular canine total hip replacement system, BioMedtrix Ltd, Allendale, NJ.

<sup>c</sup>Canine cemented total hip replacement system, Mathys, Bettlach, Switzerland.

<sup>d</sup>Canine cemented total hip replacement system, J-F Bardet, Neuilly Sur Seine, France.

<sup>e</sup>Exakt, Apparatebau GMBH, Norderstedt, Germany.

<sup>f</sup>Lumiscan 75, Lumisys Inc, Sunnyvale, Calif.

<sup>g</sup>Adobe Photoshop, Adobe Systems Inc, Mountain View, Calif.

<sup>h</sup>MacDraft, Innovative Data Design Inc, Concord, Calif.

<sup>i</sup>Kodak RFS 3570 Film Scanner, Kodak Co, Rochester, NY.

## References

1. Edwards MR, Egger EL, Schwarz PD. Aseptic loosening of the femoral implant after cemented total hip arthroplasty in dogs: 11 cases in 10 dogs (1991-1995). *J Am Vet Med Assoc* 1997;211:580-586.
2. Estok DM, Orr TE, Harris WH. Factors affecting cement strains near the tip of a cemented femoral component. *J Arthroplasty* 1997;12:40-48.
3. O'Connor DO, Burke DW, Jast M, et al. In vitro measurement of strain in the bone cement surrounding the femoral component of total hip replacements during simulated gait and stair climbing. *J Orthop Res* 1996;14:769-777.
4. Schulz KS, Vasseur P, Stover SM, et al. Transverse plane evaluation of the effects of surgical technique on stem positioning and geometry of reconstruction in canine total hip replacement. *Am J Vet Res* 1998;59:1071-1079.
5. McGrory BJ, Morrey BF, Cahalan TD, et al. Effect of femoral offset on range of motion and abductor muscle strength after total hip arthroplasty. *J Bone Joint Surg* 1995;77:865-869.
6. Ruff CB, Hayes WC. Cross-sectional geometry of pecos pueblo femora and tibiae—a biomechanical investigation: I. Method



and general patterns of variation. *Am J Phys Anthropol* 1983;60:359–381.

7. Rumph PF, Hathcock JT. A symmetric axis-based method for measuring the projected femoral angle of inclination in dogs. *Vet Surg* 1990;19:328–333.

8. Noble PC, Alexander JW, Lindahl LJ, et al. The anatomic basis of femoral component design. *Clin Orthop* 1988;235:148–164.

9. Montavon PM, Hohn RB, Olmstead ML, et al. Inclination and anteversion angles of the femoral head and neck in the dog: evaluation of a standard method of measurement. *Vet Surg* 1985;14:277–282.

10. Jasty M. Fixation by methyl methacrylate. In: Rosenberg AG, Rubash HE, eds. *The adult hip*. Philadelphia: Lippincott-Raven, 1998;187–200.

11. Andriacchi TP, Galante JO, Bebytschko TB, et al. Stress analysis of the femoral stem in total hip prosthesis. *J Bone Joint Surg* 1976;58:618–624.

12. Crowninshield RD, Brand R, Johnston RC, et al. An analysis of femoral component stem design in total hip arthroplasty. *J Bone Joint Surg* 1980;62:68–78.

13. Massat BJ, Vasseur PB. Clinical and radiographic results of total hip arthroplasty in dogs: 96 cases (1986–1992). *J Am Vet Med Assoc* 1994;205:448–454.

14. Jasty M, Webster W, Harris WH. Management of limb length inequality during total hip replacement. *Clin Orthop* 1996;333:165–171.

15. Litsky AS, Spector M. Biomaterials. In: Simon SR, ed. *Basic orthopaedic science*. Columbus: American Academy of Orthopaedic Surgeons, 1994;447–486.

16. Huiskes R, Verdura J, Verdonchot N. Biomechanics of artificial joints: the hip. In: Mow VC, Hayes WC, eds. *Basic orthopaedic biomechanics*. 2nd ed. Philadelphia: Lippincott-Raven, 1997;395–460.